

Representation and Analysis of 3D Shape

Wolfgang Heiden, Rita Cornely
Dept. of Computer Science,
FH Bonn-Rhein-Sieg – University of Applied Sciences,
Sankt Augustin, Germany
{wolfgang.heiden, rita.cornely}@fh-bonn-rhein-sieg.de

Abstract

A generic approach to describing shape and topography of arbitrary objects is presented, using linguistic variables to combine different features in one fuzzy descriptor. Although the origin of the method lies in molecular visualization and drug design, it can be applied in principle to any surface represented by a polygon mesh. Two approaches to shape description are presented that both lead to linguistic variables that can be used for surface segmentation by means of shape: One approach is based on the calculation of canonical curvatures, the other describes the “embeddedness” of a surface area related to the overall geometry of a 3D object.

Keywords: 3D shape, surface topography, fuzzy logic, linguistic variable.

1. INTRODUCTION

3-dimensional geometry in Computer Graphics is usually described either by polygon meshes or by mathematical descriptions like NURBS (non-uniform rational B-splines). The latter become quickly difficult to handle (and time-consuming to render) with increasing complexity while the former represent only a simplified approach with limited resolution to the real shape.

Several applications from Bioinformatics and Medicine demand that 3D objects (representing e.g. molecules or tissue scans) shall be segmented into parts forming a pattern of distinct relevant surface regions. Among several physico-chemical parameters shape plays a crucial role in molecular recognition. Therefore, computational chemistry has found a variety of approaches to shape classification [1]-[5].

In Computer Graphics, shape descriptors are often used to improve the quality of a polygon mesh related to the analytical surface of the original object, for feature detection, or as a first step to several geometry processing actions like deformation, texturing, storing, etc. Some recent examples use Morse theory to find implicit functions for complex surfaces [6],[7]. While these methods generally refer to *topology* (i.e. connectedness), we rather focus on *topography* as a means to describe overall shape types of a surface region (even though topography descriptors are calculated based on topological functions). Implicit functions for surface shape are usually rather complex and therefore expensive in terms of computing time. Using simple shape descriptors together with a quick yet flexible segmentation algorithm based on concepts from fuzzy logic may offer an alternative that is able to find characteristic features of polygon surfaces on varying scales.

2. DESCRIBING SHAPE

The shape of arbitrary objects is difficult to define in a general way. Even humans usually describe shape by comparing objects or parts of objects to primitives or models of known geometric parameters. A generic description of surface shape can be given in terms of curvature or – on a more global scale – by means of elevation (or embeddedness) related to some reference level, like in topographical maps. While the former (curvature) is largely dependent of the choice of scale for fitting paraboloids to surface regions of a given size (which leads to difficulties with surfaces containing shape elements of significantly varying size), the latter (embeddedness) defines shape in relation to the overall size of the measured object.

2.1 Shape descriptors based on canonical curvatures

The shape of a region around a single surface point (a mesh node) can be adequately measured by a curvature profile based on the two canonical curvatures (CC1, CC2), which are originally defined as the eigenvalues of the local Hessian matrix. For larger surface areas, *global curvatures* have been introduced, which are calculated analogously by fitting paraboloids to a central node point and its neighbours bordering a surrounding area at a predefined distance following node connectivities [2].

For a simple representation of surface shape a Surface Topography Index (STI) has been defined [8],[9], assigning a characteristic number to every node point of a triangular mesh as a regional shape descriptor. The STI combines both canonical curvatures in a single scalar value as the continuous transition between five characteristic shape types (bag, cleft, saddle, ridge, knob), as depicted in Figure 1.

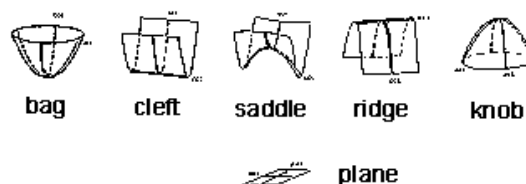


Figure 1: Characteristic shapes from combination of canonical curvatures.

With $CC1 > CC2$ the STI can be calculated as follows:

$$\begin{aligned}
\text{STI} &= (\text{CC1}-\text{CC2}) / \text{CC1} && \rightarrow \textit{bag to cleft} \\
&&& \text{if } (\text{CC1}>0 \text{ and } \text{CC2}>0) \\
\text{STI} &= 1 + 1 - (\text{CC1}+\text{CC2}) / \text{CC1} && \rightarrow \textit{cleft to saddle} \\
&&& \text{if } (\text{CC1}>0 \text{ and } \text{CC2}\leq 0 \\
&&& \text{and } |\text{CC1}| > |\text{CC2}|) \\
\text{STI} &= 2 + (\text{CC1}+\text{CC2}) / \text{CC2} && \rightarrow \textit{saddle to ridge} \\
&&& \text{if } (\text{CC1}>0 \text{ and } \text{CC2}\leq 0 \\
&&& \text{and } |\text{CC1}| \leq |\text{CC2}|) \\
\text{STI} &= 3 + 1 - (\text{CC2}-\text{CC1}) / \text{CC2} && \rightarrow \textit{ridge to knob} \\
&&& \text{if } (\text{CC1}\leq 0 \text{ and } \text{CC2}<0) \\
\text{STI} &= -1 && \rightarrow \textit{plane} \\
&&& \text{if } (\text{CC1} = \text{CC2} = 0)
\end{aligned}$$

The STI (except for the special case of a plane) varies continuously from 0 to 4:

$$0 \leq \text{STI} \leq 4$$

Duncan and Olson [4],[5] have defined a similar – but analytically continuous – Shape Index s with :

$$s = -\frac{2}{\pi} \arctan \frac{\text{CCI} + \text{CC2}}{\text{CCI} - \text{CC2}}$$

where $-1 \leq s \leq +1$

It has been shown [10] that s and STI, when mapped on a surface as colour code, lead to virtually identical results.

In addition, the Curvedness R of a surface can be calculated as well from the canonical curvatures [4],[5]:

$$R = \sqrt{\frac{1}{2}(\text{CCI}^2 + \text{CC2}^2)}$$

2.2 Topography descriptor based on surface embeddedness

In our daily experience there is another, very simple and equally intuitive, representation of shape in terms of topography of a landscape. Positive or negative elevation with regard to a reference level is quantified and can be represented by a colour code on a topographical map. Although landscape topography is usually considered as planar-based, it is in fact related to a globular 3D object, the earth. Analogously to this globe, the local variation of topography of any 3D geometry can be understood as elevation or embeddedness of a surface region with regard to the interior enclosed by the surface of the object.

A simple method to define such an “embeddedness potential” comes from molecular surface visualization.

2.2.1 Molecular Surfaces

Molecules are aggregates of atoms, held together by several interatomic forces. Although, strictly speaking from the quantum physical view, molecules do not really have a surface in the

macroscopic sense, they often behave as if they did. This empirical observation can be explained and (approximately) quantified by the Lennard-Jones (12,6) Potential that defines the van der Waals radii of atoms [11]. On this basis, Connolly defined solvent accessible molecular surfaces by rolling a probe sphere over the van der Waals surface of molecules [12]. Molecular surfaces can then be represented as triangular meshes [13],[14].

2.2.2 Surface Embeddedness Potential

When looking for a pseudo-potential adequately describing local lipophilicity on molecular surfaces, it was found that earlier lipophilicity potentials considering distance-dependent atomic contributions suffered from massive influence of topography [15]. Depriving these potentials from the lipophilicity part lead to a distance dependency of $1/(1+d_i)$ with d_i being the distance of atom i from the surface node for which the potential shall be calculated. Replacing $1/(1+d_i)$ by $1/(1+d_i^2)$ leads to a sharper cut between the contribution of closer and farther located atoms. The resulting Surface Embeddedness Potential (SEP) for the surface of a molecule built of N atoms is defined as follows:

$$\text{SEP} = \sum_{i=1}^N \frac{1}{1+d_i^2}$$

The SEP is shown in Figure 2.

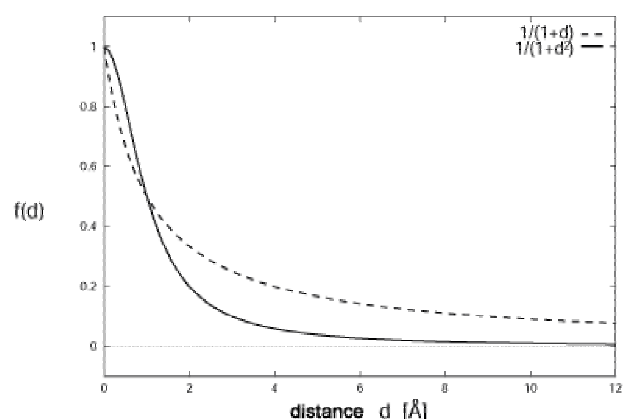


Figure 2: Surface embeddedness potential functions.

Figure 3 illustrates what the SEP really means in terms of topography. The potential value increases with the number of atoms in close distance to the regarded surface point, thus giving an impression of how close a point on a polygon mesh is to the bulky interior of the enclosed volume.

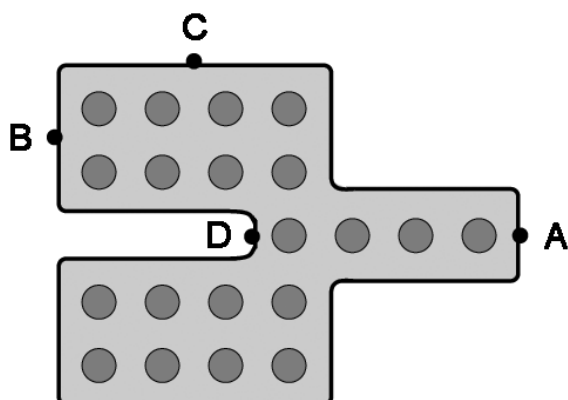


Figure 3: Surface embeddedness. The internal space of the object is filled with atoms (large circles). Surface points (small numbered circles) are increasingly embedded from A to D, according to the number and distance of nearby atoms:

$$f(A) < f(B) < f(C) < f(D)$$

2.2.3 Generalizing 3D Surface Topography

Since the SEP has been defined for molecular surfaces, it carries some inherent features that don't apply to all surfaces in general. First, the scale of molecules is always identical. Therefore it makes sense to calculate an absolute embeddedness value that can be compared to that of other molecules, even if they differ considerably in size. For a general embeddedness representation of surfaces of arbitrary scale the SEP should be normalized:

$$SEP_n = \frac{\sum_{i=1}^N \frac{1}{1+d_i^2}}{N}$$

Second, the SEP is defined by a distance-dependent contribution of atoms which are always in defined spatial relationship to molecular surfaces but not to macroscopic geometries. However, polygon meshes resembling molecular surfaces can be generated by blobby-type models, where the blob centers replace the atom coordinates [16]. Unfortunately, in this case we would again face the problem of finding an implicit function for the surface which could reconstruct the blob centers.

A less accurate but much simpler solution may be found by filling the interior of the object with a regular grid of artificial pseudo-atoms. Close to the surface, however, in this case the results will not be clearly defined, as there is no general surface-related for positioning the grid. This effect should be reduced with an increasing number of grid points.

Another approach is to use the surface polygons themselves instead of atoms, scaled with their area as some kind of "mass" measure:

$$SEP' n = \frac{\sum_{i=1}^N \frac{1}{1+a_i \cdot d_i^2}}{\sum_{i=1}^N a_i}$$

with a_i = area of polygon i and d_i = distance to (reference point of) polygon i . In this case the resulting value would, however, represent depth or height as an absolute value rather than embeddedness or elevation, since the contribution of bulk surface polygons of a large object to embedded surface regions (where the distance of most of these polygons might well be beyond the cutoff) would often be negligible. Still, together with a shape descriptor (like STI or Shape index s) that gives information of the direction related to the reference surface, also the SEP n value could help to better distinguish the shape of different surface regions.

Overall the SEP may not be ideal for quantitative comparison of surfaces, but it is well suited for segmentation of a surface by means of topography.

3. FUZZY SURFACE SEGMENTATION

When analyzing molecular surfaces one usually looks for locations of intermolecular interaction. The lock-and-key model postulates that (together with physical properties) local shape complementarity is a prerequisite for interaction, in particular regarding the initial contact referred to as *docking*. There are several approaches to molecular docking simulations based on shape descriptors [3],[17]. As an initial step to modular docking simulation surfaces can be segmented into domains by means of local surface potentials including shape. As a flexible method for this segmentation a region growth algorithm based on the dissimilarity of linguistic variables has been introduced [3]. Based on this method docking simulations could be successfully conducted [17].

3.1 Fuzzy Set Theory

The theory of fuzzy sets [18],[19] can be regarded as a generalization of the classical set theory, with each element of a fuzzy set \tilde{A} consisting of a pair of values, where each value of a basic variable x (comparable to an element of a classical – „crisp“ – set) in the definition area X is assigned a membership function value $\mu_{\tilde{A}}(x)$ that gives the grade of membership of that element to the set \tilde{A} :

$$\tilde{A} = \left\{ (x, \mu_{\tilde{A}}(x)) \mid x \in X \right\} \quad \text{with (usually):} \quad 0 \leq \mu_{\tilde{A}}(x) \leq 1$$

3.2 Linguistic Variables

A core feature of fuzzy logic is the use of *Linguistic Variables* (LV) [20] instead of the crisp variables of classical mathematics. These are groups of fuzzy sets with more or less overlapping membership functions (usually – but not necessarily) over an identical basic variable. The fuzzy sets of a LV are semantically related and can be interpreted as classes or categories within the LV. A linguistic variable L with n classifying fuzzy sets \tilde{A} can generally be defined as follows:

$$L = \{ \tilde{A}_1, \dots, \tilde{A}_n \} \quad \text{or} \\ L = \left\{ (x, \mu_{\tilde{A}_1}(x)), \dots, (x, \mu_{\tilde{A}_n}(x)) \right\}$$

After numerical values have been transformed to linguistic variables (fuzzification), rules defined in a fuzzy way can easily be applied. This is usually done by combination of different linguistic variables with various operators which produce new linguistic variables from old ones. However, for segmentation of molecular surfaces we chose another method by calculating the dissimilarity of two linguistic variables.

3.3 Fuzzy Dissimilarity

Similarity and dissimilarity play a crucial role in pattern recognition. The terms themselves are inherently fuzzy. The dissimilarity D_{LV} of two linguistic variables A, B of identical type has been defined as follows [8]:

$$D_{LV}(A, B) = \frac{\sum_{i=1}^n w_i |\mu_{\tilde{A}_i}(x) - \mu_{\tilde{B}_i}(x)|}{\sum_{i=1}^n w_i (\mu_{\tilde{A}_i}(x) + \mu_{\tilde{B}_i}(x))}$$

with

$$A = \{(x, \mu_{\tilde{A}_1}(x)), \dots, (x, \mu_{\tilde{A}_n}(x))\}$$

$$B = \{(x, \mu_{\tilde{B}_1}(x)), \dots, (x, \mu_{\tilde{B}_n}(x))\}$$

$$0 \leq \mu_{\tilde{A}_i}, \mu_{\tilde{B}_i} \leq 1$$

$$0 \leq w_i \leq 1$$

w_i = weighting factor for category i

n = number of categories in A, B

where

$$0 \leq D_{LV}(A, B) \leq 1$$

Weighting factors allow for fine-tuning of the dissimilarity function based on the importance of different categories for the overall comparison.

The similarity S_{LV} of these linguistic variables can easily be derived from D_{LV} :

$$S_{LV} = 1 - D_{LV}$$

3.4 Surface Segmentation

Segmentation of a surface based on linguistic variables can be performed with a region growth method where domains are started at a prominent node point, growing along the polygon mesh until the dissimilarity between the regarded LV at the next node and the average LV of the domain so far exceeds a given limit or until the border of an already defined domain is reached [8].

Before segmentation can be performed, fuzzification is required, i.e. the transformation of a scalar into a linguistic variable. Since STI is defined by continuous deformation over 5 characteristic shapes (plus the special case of a plane), fuzzification as depicted in Figure 4 seems reasonable. For SEP a more simple fuzzification is sufficient (see Figure 5).

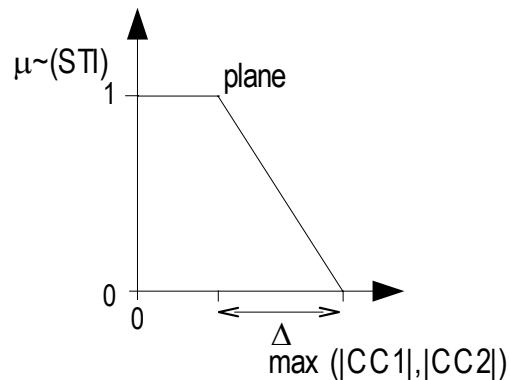
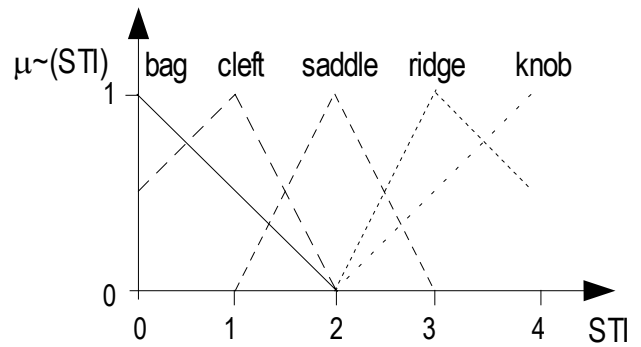


Figure 4: STI fuzzification. 5 categories are derived directly from STI, the 6th (plane) from the maximum absolute of both canonical curvatures (CC1, CC2).

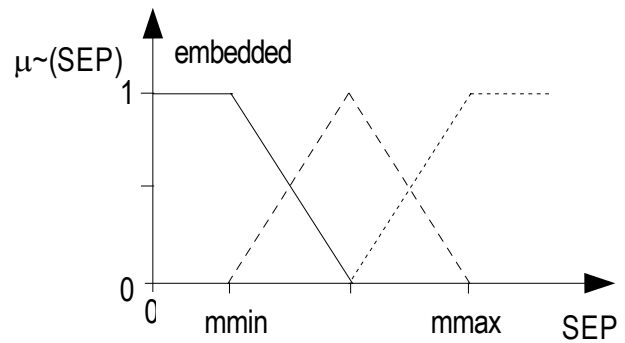


Figure 5: SEP fuzzification.

Fuzzy segmentation is tolerant towards sub-optimal choice of the starting point (see Figure 6), which makes it very well suited for the segmentation of complex surfaces.

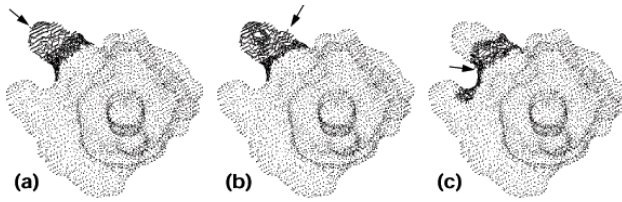


Figure 6: Fuzzy segmentation of a complex surface by a LV representation of STI. Starting a domain at an elevation top (a) leads to almost identical results also starting at any point within the domain (b). Only a starting point close to the domain edge (c) results in considerably different segmentation.

4. EXAMPLE

For a better understanding of the procedure a schematical example shall illustrate what happens to a simple polygon surface in the shape analysis and segmentation process.

Consider a sample polygon (triangle) surface (see fig. 7) consisting of a somehow globular bulk, a protrusion with almost circular cross-section (a), an equally circular but less deep hole (b), and a long and deep cleft (c).

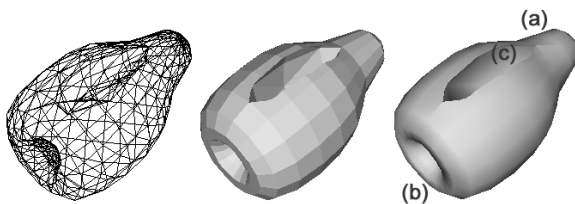


Figure 7: Sample surface with protrusion (a), intrusion (b), and cleft (c).

4.1 Curvature calculation

In a first step two global canonical curvatures are calculated for every triangle node point of the surface by fitting two perpendicular paraboloids (with the tip at the respective surface node) to a region of pre-defined size according to the (shortest) distance from the node point following the mesh edges [2]. The pre-defined distance is a measure of globality for detecting curvatures on the surface. This procedure would generate a set of two values for each node point. These two values would both be of similar size for regions (a) and (b), both with equal negative or positive sign, respectively. In region (c) the curvature calculation would yield two positive (i.e. concave) values of different size for the long and cross section of the cleft.

4.2 STI calculation

Once the regional canonical curvatures are known for each node, the STI can be calculated (see 2.1). At the tip of region (a) the value would be close to 4 (“knob”), at the tip of region (b) close to 0 (“bag”), along the inner line of region (c) close to 1 (“cleft”), and on the bulky rest somewhere between 3 and 4 (“ridge” to “knob”) because of the global convex shape of the sample object. Between the extreme positions the STI would vary continuously with the changing relationship of the canonical curvatures to each other.

4.3 SEP calculation

As an alternative shape definition to STI or as a supplement which yields information about depth relative to the global object bulk, the SEP (see 2.2.2) can be calculated if “pseudo-atom” objects are placed within the sample surface (see fig. 8).



Figure 8: Sample surface (transparent) with a pseudo-atom grid inside.

The SEP value of each surface node depends on the number and vicinity of nearby “atoms”. High SEP values are achieved if many atoms are close (which is the case for the tip of region (b) – the “bag” – and deep inside region (c) – the “cleft”). Low SEP values stand for regions far extruded from the surface bulk, e.g. the tip of region (a) – the “knob”. The highest values would be found at the low edges of region (c) as they are enclosed at three sides and deeper engraved in the bulk than the “bag” region (b).

4.4 Fuzzy segmentation

Segmentation of the polygon surface is possible based on either STI or SEP (or a combination of both). First, fuzzification of the basis variable(s) leads to a vector filled with scalar values (representing the membership function values of the according linguistic variable – LV) for every surface node.

Segmentation starts at a node where the basis variable is extreme, e.g. at the tip of the “nob” region (a). The LV of this node (currently representing the segment) is then compared to the LV of its nearest neighbor node which is not yet assigned to a segment, using the Dissimilarity function given in 3.3. As long as the dissimilarity value does not exceed a given limit, the new node is added to the current segment and a new average segment LV is calculated before continuing with the nearest neighbor of this new node. Else the region growth stops here, going back to the last segment node which still has free neighbors. A segment is finished when no new nodes can be added either because all node neighbors are already assigned to a segment (including the current one) or excluded because of dissimilarity. Then the procedure starts anew with an extreme surface node not yet assigned to any segment, until no free node is left.

In case of our sample surface fuzzy segmentation by STI would lead to a set of surfaces like shown in fig. 9.

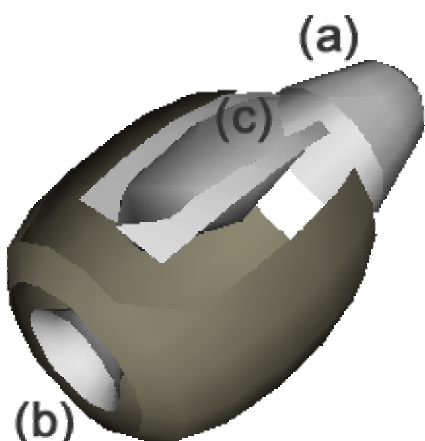


Figure 9: Sample surface segmented by shape with segments: (a) nob, (b) bag, (c) cleft plus the (darker) bulky rest.

5. APPLICATIONS

The method (or rather: combination of methods) can be used to help find significant differences in the shape of similar complex surfaces, when these differences are expected to be important though they are far from being obvious. Examples can be seen in fig. 10-11.

Figure 10 shows the result of a segmentation of the surfaces of three digestive proteins by SEP, where the specificity pocket of each protein was extracted automatically, obviously showing their different shape which is responsible for variations in specificity of these closely related enzymes (catalytic proteins).

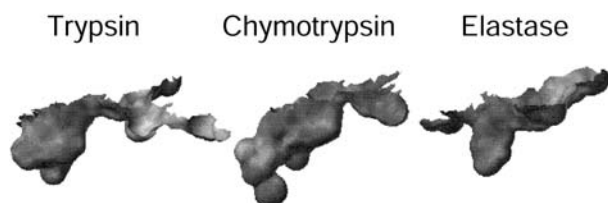


Figure 10: Specificity pockets of three digestive enzymes, extracted automatically from the protein surfaces by fuzzy segmentation via SEP.

Figure 11 shows the surfaces of two proteins, the digestively active trypsin and its inactive predecessor trypsinogen. Both surfaces are not obviously different. Yet when comparing only the concave segments it can be easily seen that there is only one significant difference (which is in fact responsible for the activation of the enzyme). The figure illustrates the ability of the described procedure to identify similarly shaped regions of different complex surfaces.

Parts of the features described here are integrated in the molecular modeling and visualization software MOLCAD [21].

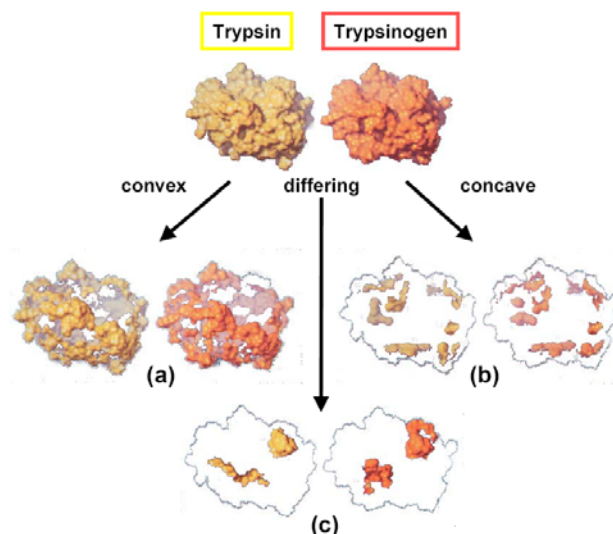


Figure 11: Specificity pockets of the digestive enzyme trypsin (left) and its inactive predecessor trypsinogen (right). Segmentation by STI yields a convex bulk (a) and a number of practically identical concave domains (b) plus one significantly different concave domain (c). A single additional apparently different convex domain is obviously not significant but rather due to the different origin of the surface models together with the fuzzy segmentation procedure.

6. CONCLUSION AND OUTLOOK

Exner et al. combined Shape Index and Curvedness, together with physico-chemical parameters in fuzzy docking simulations [17]. In molecular classification (e.g. for categorization of pharmaceutical compounds) a similar approach could prove helpful, integrating STI and SEP in a linguistic variable that may contain categories like “deep cleft” or “rather flat nob”.

It has been shown that STI (or Shape Index) and SEP give a consistent representation of shape and topography of polygon surfaces, respectively. Although there is much redundancy, both values contain information not present in each other. SEP, for example, gives an impression of the depth of a particular shape element (e.g. a bag-type domain).

A combined fuzzy representation of generic surface shape descriptors may also open the door to other applications like automatic shape feature recognition of 3D objects.

7. ACKNOWLEDGEMENT

This work is supported by Tripos Inc., St. Louis, USA.

8. REFERENCES

- [1] Mezey, P. G.: Global and local relative convexity and oriented relative convexity: application to molecular shapes in external fields. *J. Math. Chem.* **2** (1988), 325-346.
- [2] Zachmann, C.-D., Heiden, W., Schlenkrich, M., Brickmann, J.: Topological Analysis of Complex Molecular Surfaces. *J. Comp. Chem.* **13**, 1 (1992), 76-84.

- [3] Shoichet, B., Bodian, D., Kuntz, I.: Molecular Docking Using Shape Descriptors. *J.Comp.Chem* **13**, 3 (1992), 380-397.
- [4] Duncan, B. S., Olson, A. J.: Approximation and Characterization of Molecular Surfaces. *Biopolymers* **33** (1993), 219-229.
- [5] Duncan, B. S., Olson, A. J.: Shape Analysis of Molecular Surfaces. *Biopolymers* **33** (1993), 231-238.
- [6] Hart, J.: Computational Topology for Shape Modeling. *Proc. Shape Modeling International '99*, IEEE CS (1999), 36-45.
- [7] Ni, X., Garland, M., Hart, J. : Fair Morse Functions for Extracting the Topological Structure of a Surface Mesh. *Proc. SIGGRAPH '04* (2004).
- [8] Heiden, W., Brickmann, J.: Segmentation of protein surfaces using fuzzy logic. *J. Mol. Graphics* **12** (1994), 106-115.
- [9] Brickmann, J., Heiden, W., Vollhardt, H., Zachmann, C.-D.: New Man-Machine Communication Strategies in Molecular Modelling. in: *Proceedings of the Twenty-Eighth Annual Hawaii International Conference on System Sciences* , L. Hunter, B.D. Shriver, Eds., IEEE Computer Society press, Los Alamitos, CA., (1995), 273-282.
- [10] Exner, T.: Computergestützte Strukturbestimmung biochemischer Komplexe durch einen *Fuzzy Logic*-basierten Algorithmus. *PhD Thesis, TU Darmstadt* (2000)
- [11] Bondi, A.: van der Waals Volumes and Radii. *J. Phys. Chem.* **68** (1964), 441-451.
- [12] Connolly, M.: Solvent Accessible Surfaces of Proteins and Nucleic Acids. *science* **221** (1983), 709-713.
- [13] Heiden, W., Schlenkrich, M., Brickmann, J.: Triangulation Algorithms for the Representation of Molecular Surface Properties. *J. Comp.-Aided Mol. Design* **4** (1990), 255-269.
- [14] Heiden, W., Goetze, T., Brickmann, J. : Fast Generation of Molecular Surfaces from 3D Data Fields With an Enhanced 'Marching Cube' Algorithm. *J. Comp. Chem.* **14**, 2 (1993), 246-250.
- [15] Heiden, W., Moeckel, G., Brickmann, J.: A new approach to analysis and display of local lipophilicity/ hydrophilicity mapped on molecular surfaces. *J. Comp.-Aided Mol. Design* **7** (1993), 503-514.
- [16] Blinn, J.: A Generalization of Algebraic Surface Drawing. *ACM Transactions on Graphics* **1**, 3 (1982), 235-256.
- [17] Exner, T. E.; Brickmann, J.: Molecular Shape Recognition Using Fuzzy Logic Strategies, *Match - Communications in Mathematical and in Computer Chemistry* **38** (1998), 53-80.
- [18] Zadeh, L. A.: Fuzzy sets. *Information and Control* **8** (1965), 338-353.
- [19] Zimmermann, H.-J.: Fuzzy Set Theory - and Its Applications. Kluwer, Boston (1991).
- [20] Zadeh, L. A.: The concept of a linguistic variable and its application to approximate reasoning. Memorandum ERL-M 411 Berkeley (October 1973).
- [21] Brickmann, J., Goetze, T., Heiden, W., Moeckel, G., Reiling, S., Vollhardt, H., Zachmann, C.-D.: Interactive Visualization of Molecular Scenarios with MOLCAD/SYBYL. in: *Data Visualisation in Molecular Science: Tools for Insight and Innovation*, Bowie (ed.), J.E. Reading, Mass. Addison-Wesley Publishing Company Inc. (1995), 83-97.

About the authors

Wolfgang Heiden is a professor at FH Bonn-Rhein-Sieg, Department of Computer Science. His contact email is wolfgang.heiden@fh-bonn-rhein-sieg.de.

Rita Cornely is a PhD student at FH Bonn-Rhein-Sieg, Department of Computer Science and University Bonn, Inst. for Pharmaceutical Chemistry. Her contact email is rita.cornely@fh-bonn-rhein-sieg.de.